J|A|C|S
ARTICLES
Published on Web 03/23/2007

Site- and Orientation-Selective Anchoring of a Prototypical Molecular Building Block

Pascal Ruffieux,*,† Krisztián Palotás,‡ Oliver Gröning,† Daniel Wasserfallen,£ Klaus Müllen,£ Werner A. Hofer,‡ Pierangelo Gröning,† and Roman Fasel†

Contribution from the Empa, Swiss Federal Laboratories for Materials Testing and Research, Feuerwerkerstrasse 39, 3602 Thun, Switzerland, Surface Science Research Center, University of Liverpool, Liverpool L69 3BX, Britain, and Max-Planck-Institute for Polymer Research, Ackermannweg 10, 55128 Mainz, Germany

Received October 18, 2006; Revised Manuscript Received February 7, 2007; E-mail: pascal.ruffieux@empa.ch

Abstract: The controlled anchoring of molecular building blocks on appropriate templates is a major prerequisite for the rational design and fabrication of supramolecular architectures on surfaces. We report on a particularly selective adsorption process of hexa-peri-hexabenzocoronene on Au(111), which leads to well-controlled adsorption position and orientation of the polycyclic aromatic hydrocarbons. Scanning tunneling microscopy reveals selective adsorption on monatomic steps in the fcc stacking regions with a specific orientation of 18° between the molecular axis and the step normal. Ab initio calculations for various adsorption sites reveal the lowest total energy for adsorption on a kink site. Energy considerations and the excellent agreement between experimental and simulated images show that adsorption on kink sites is responsible for the specific adsorption angle.

Introduction

The aim to build functional supramolecular structures by self-assembly has recently spawned a large number of investigations on molecular structures in solution as well as at surfaces.[1] Regarding self-assembly at surfaces, the basic requirements are (i) the preparation of substrate surfaces acting as appropriate templates for supramolecular structures and (ii) the design of appropriate molecular building blocks incorporating functional groups. The molecular core in this case enforces the adsorption at predefined sites of the surface, while the functional groups remain accessible for bonding with a postdeposited second type of molecule. Considerable progress has been made with respect to (i) by the use of surface reconstruction patterns,[2] structures evolving from lattice mismatch,[3,4] and vicinal surfaces[5] to produce periodically modulated surfaces with large unit cells. However, only a few investigations of supramolecular pattern formation on such template structures have been reported.[6,7]

Polycyclic aromatic hydrocarbons (PAHs) based on the structure of hexa-peri-hexabenzocoronene (HBC, $C_{42}H_{18}$) have attracted considerable attention due to their large structural variety offering the possibility of accommodating different symmetry functional groups.[8−10] The choice of appropriate functional groups allows one to tune the ratio between intermolecular and molecule−substrate interactions, which is a crucial parameter for the control of self-assembly. Recent studies further showed the possibility of controlling the charge state of the core by attaching charge-transfer complexes to the HBC molecule, resulting in a prototypical single-molecule chemical-field-effect transistor.[11]

Here, we report on a successful site- and orientation-selective anchoring of HBC on monatomic steps of a gold surface where the orientation selectivity results from a specific interaction between the molecule and the step edge. The exact adsorption site and orientation is determined by low-temperature scanning tunneling microscopy (STM) combined with ab initio density functional theory (DFT) and electron-transport calculations.

Experimental Section

Experiments were performed in ultrahigh vacuum (base pressure of 5×10^{-11} mbar) using a low-temperature scanning tunneling microscope.[12] The Au(111) surface was prepared by several cycles of Ar^+ ion sputtering and subsequent annealing to 700 K. The synthesis of HBC is described elsewhere.[13] Molecules were deposited via vacuum

† Swiss Federal Laboratories for Materials Testing and Research.
‡ University of Liverpool.
£ Max-Planck-Institute for Polymer Research.

(1) Whitesides, G. M.; Grzybowski, B. *Science* **2002**, *295*, 2418−2421.
(2) Yokoyama, T.; Yokoyama, S.; Kamikado, T.; Okuno, Y.; Mashiko, S. *Nature* **2001**, *413*, 619−621.
(3) (a) Brune, H.; Giovannini, M.; Bromann, K.; Kern, K. *Nature* **1998**, *394*, 451−453. (b) Brune, H. *Surf. Sci. Rep.* **1998**, *31*, 121−229.
(4) Corso, M.; Auwärter, W.; Muntwiler, M.; Tamai, A.; Greber, T.; Osterwalder, J. *Science* **2004**, *303*, 217−220.
(5) Rousset, S.; Repain, V.; Baudot, G.; Garreau, Y.; Lecoeur, J. *J. Phys.: Condens. Matter* **2003**, *15*, S3363−S3392.
(6) Néel, N.; Kröger, J.; Berndt, R. *Adv. Mater.* **2006**, *18*, 174−177.
(7) Vladimirova, M.; Stengel, M.; Vita, D. A.; Baldereschi, A.; Böhringer, M.; Morgenstern, K.; Berndt, R.; Schneider, W. D. *Europhys. Lett.* **2001**, *56*, 254−260.
(8) (a) Samori, P.; Severin, N.; Simpson, C. D.; Müllen, K.; Rabe, J. *J. Am. Chem. Soc.* **2002**, *124*, 9454−9457. (b) Wang, Z.; Dötz, F.; Enkelmann, V; Müllen, K. *Angew. Chem.* **2005**, *117*, 1273−1276.
(9) Ruffieux, P.; Gröning, O.; Fasel, R.; Kastler, M.; Wasserfallen, D.; Müllen, K.; Gröning, P. *J. Phys. Chem. B* **2006**, *110*, 11253−11258.
(10) Gross, L.; Moresco, F.; Ruffieux, P.; Gourdon, A.; Joachim, C.; Rieder, K. H. *Phys. Rev. B* **2005**, *71*, 165428-1−165428-7.
(11) Jäckel, F.; Watson, M. D.; Müllen, K.; Rabe, J. P. *Phys. Rev. Lett.* **2004**, *92*, 188303-1−188303-4.
(12) Omicron Nanotechnology GmbH, D-Taunusstein.

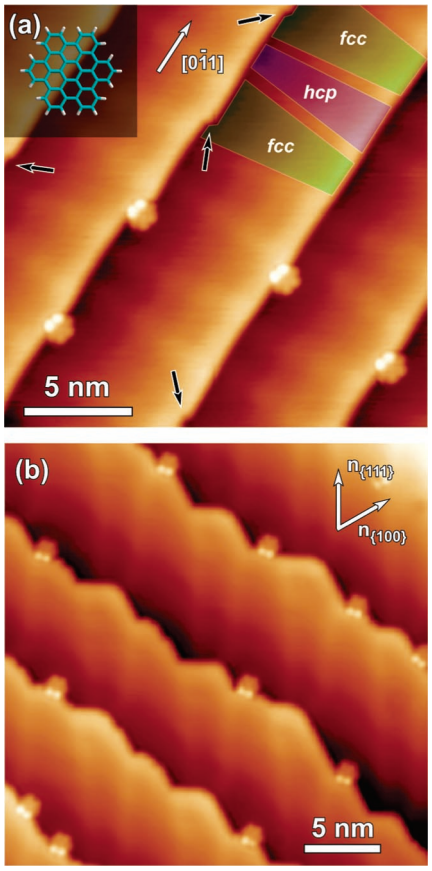

Figure 1. STM topography images ($U = 0.5$ V, $I = 0.05$ nA) of HBC adsorbed on Au(111) at low coverage (~0.05 ML). (a) STM image of an area with steps running along the [0$\bar{1}$1] direction. Black arrows indicate the position of unoccupied kink sites. The inset shows the structural model of HBC. (b) STM image of an area with alternating step directions.

sublimation from a quartz crucible (Kentax, TCE−BSC) heated to 700 K with the sample kept at room temperature. A quartz microbalance was used for thickness calibration. Subsequently, the sample was cooled to 5 K directly in the STM chamber.

In order to gain a detailed understanding, the experimental STM results were compared to ab initio simulations based on DFT calculations,[14] which have been performed using VASP[15] in its generalized gradient approximation (GGA). For the description of the ionic cores, we used ultrasoft pseudopotentials. The STM images have been calculated with bSKAN,[14] a highly efficient and flexible software package designed to describe electron transport through a vacuum barrier. The theoretical model is based on multiple scattering theory.[16]

Results and Discussion

X-ray photoelectron diffraction measurements reveal that, at full monolayer coverage, HBC molecules adsorb in a flat-lying configuration on Au(111) with the C−C bond direction along [0$\bar{1}$1].[17] In the present work, we have investigated the adsorption of HBC on Au(111) at very low coverage, which allows determination of the energetically favorable adsorption site in the absence of intermolecular interactions. Figure 1 shows STM images taken at a coverage of ~0.05 monolayers (ML) in areas of high step density. The bright lines on terraces are due to discommensuration lines, which derive from the $22 \times \sqrt{3}$ reconstruction of the Au(111) surface.[18,19] These are ridges of surface atoms occupying bridge sites, which separate the larger face-centered cubic (fcc) and the smaller hexagonal close-packed (hcp) stacking regions.[19]

For room-temperature deposition, molecules are mobile on the terraces and diffuse to their preferred adsorption site at step edges where they are immobilized, as revealed by STM measurements at room temperature. This observation is in line with low-coverage investigations of HBC adsorbed on a Cu(111) surface, showing that step decoration is completed before individual molecules are present on the free terrace.[10] By contrast, deposition experiments with the sample kept at 10 K (not shown) result in a stochastic distribution of the molecules, indicating a largely suppressed mobility at low temperatures.

For room-temperature deposition, step edges are only decorated in the fcc stacking regions, while no adsorption is observed in the hcp regions, indicating an increased binding energy at step edges in fcc regions. This can be understood on the basis of a different electronic potential, reported to be 25 meV higher for fcc regions than that for hcp regions of the Au(111)$-22 \times \sqrt{3}$ superstructure, which influences the respective adsorption energies.[20] A similar selective decoration has been observed for the adsorption of C_{60}[21] and 1-nitronaphthalene.[7]

STM images of molecules adsorbed at step edges deviate significantly from the planar shape recorded for molecules adsorbed on the flat terrace. The two aromatic rings pointing to the upper terrace appear 1.2 Å higher than the lower part of the molecule (Figure 2). Given that STM is sensitive to the local electron density, this raises the question whether the apparent asymmetric shape of the molecule is related to a topographic or to an electronic effect. We will show that both the origin of the asymmetry as well as the particular angle between the mirror plane of the molecule and the step edge are topographical effects related to the adsorption site of the molecule.

HBC, with its hexagonal footprint in STM images, allows a direct assignment of the azimuthal orientation of the molecules.[9] This has been used to statistically characterize the distribution of azimuthal orientations of molecules adsorbed at step edges. Figure 3 shows a large-scale image recorded in a region with a high density of monatomic steps. The average step direction deviates from the close-packed [0$\bar{1}$1] direction by ~10°. Accordingly, straight parts of the steps running along [0$\bar{1}$1] are intersected by frequent kink sites and small parts of close-packed steps oriented along the [$\bar{1}$01] direction. Geometrically, the difference between the two close-packed step directions, with a relative orientation of 60°, is given by different microfacets defined by the outermost atom row of the upper terrace and the subsequent row on the lower terrace. Steps along the [0$\bar{1}$1] and the [$\bar{1}$01] direction define {111} and {100} microfacets, respectively.[5]

We determined the distribution of molecular orientations by comparing scan areas containing a single molecule with a

(13) Iyer, V. S.; Wehmeier, M.; Brand, J. D.; Keegstra, M. A.; Müllen, K. *Angew. Chem.* **1997**, *109*, 1676−1679.
(14) Hofer, W. A. *Prog. Surf. Sci.* **2003**, *71*, 147−183.
(15) Kresse, G.; Furthmüller, J. *Phys. Rev. B* **1996**, *54*, 11169−11186.
(16) Palotás, K.; Hofer, W. A. *J. Phys.: Condens. Matter* **2005**, *17*, 2705−2713.
(17) Ruffieux, P.; Gröning, O.; Bielmann, M.; Simpson, C.; Müllen, K.; Schlapbach, L.; Gröning, P. *Phys. Rev. B* **2002**, *66*, 073409-1−073409-4.
(18) (a) Harten, U.; Lahee, A. M.; Toennies, J. P.; Wöll, Ch. *Phys. Rev. Lett.* **1985**, *54*, 2619−2622. (b) Wöll, Ch.; Chiang, S.; Wilson, R. J.; Lippel, P. H. *Phys. Rev. B* **1989**, *39*, 7988−7991.
(19) Barth, J. V.; Brune, H.; Ertl, G.; Behm, R. J. *Phys. Rev. B.* **1990**, *42*, 9307−9318.
(20) Chen, W.; Madhavan, V.; Jamneala, T.; Crommie, M. F. *Phys. Rev. Lett.* **1998**, *80*, 1469−1472.
(21) Xiao, W.; Ruffieux, P.; Ait-Mansour, K.; Gröning, O.; Palotás, K.; Hofer, W. A.; Gröning, P.; Fasel, R. *J. Phys. Chem. B* **2006**, *110*, 21394−21398.

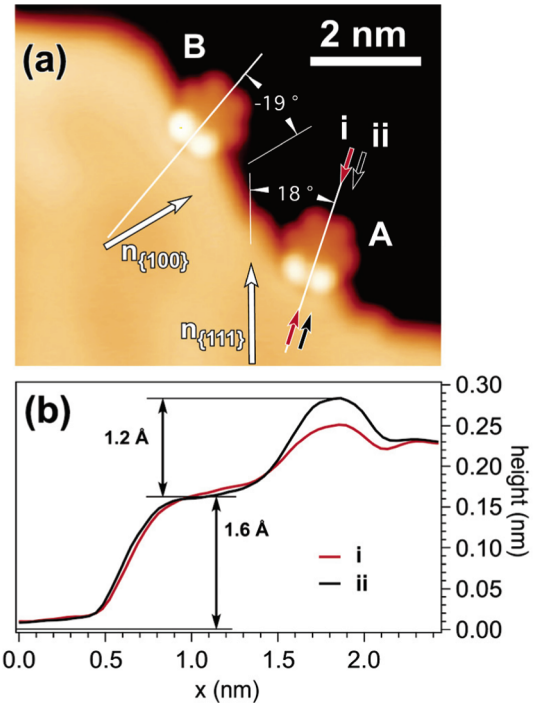

Figure 2. (a) High-resolution image ($U = 0.2$ V, $I = 0.1$ nA) of two molecules adsorbed at a monatomic step edge. Directions normal to the {111}- and the {100}-facetted steps are indicated. The discommensuration lines related to the herringbone reconstruction run in the vertical direction. (b) Line profiles along paths indicated in (a) revealing the apparent height along the molecular mirror axis (i) and over the height maximum (ii).

reference molecule, and a reliability (R) factor analysis. The R factor is determined by a least-square fit of the two images, with the relative lateral offset and angle of the molecule as free-fit parameters. In order to avoid contributions of the local topography of the metal step edge, only the orientation of the two upper aromatic rings is analyzed by selecting the uppermost part of the local height histogram (Figure 3c). The orientational distribution of the ~100 molecules adsorbed within the scan range is shown in Figure 3b. It shows a pronounced maximum centered at 18° with respect to the normal of the step along the $[0\bar{1}1]$ direction. Only two molecules are found to exhibit a different orientation, which, however, turns out to have the same offset angle with respect to the other close-packed step direction running along $[\bar{1}01]$. The relative occupancy of the two possible molecular orientations varies with the mean step direction. However, the relative angle of 18° with respect to the normal of close-packed steps is observed to be independent of the average step direction, revealing a highly selective adsorption behavior.

From the ~250 molecules analyzed with respect to their adsorption site and molecular orientation, we find, first, that all molecular orientations are comprised within a narrow distribution (fwhm = 4°) centered at 18° with respect to the close-packed row directions and, second, that 96% of the molecules are adsorbed within fcc stacking regions and 4% on the discommensuration lines. No molecules are adsorbed in hcp stacking regions.

A single molecular orientation is obtained for steps along the $[0\bar{1}1]$ direction (Figure 1a). For such steps, the molecular axis is oriented at ±18° with respect to the step normal. The sign of the angle depends on the type of kinks present along

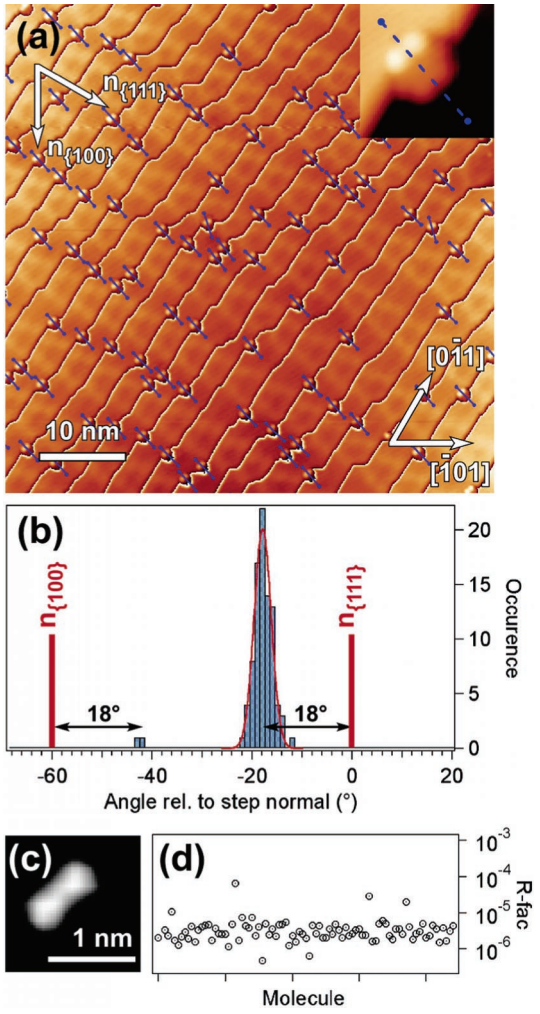

Figure 3. R-factor analysis of molecular orientation. (a) Large area topography image ($U = 0.1$ V, $I = 0.03$ nA). The corrugation due to the step edges has been subtracted in order to enhance contrast on the molecules and discommensuration lines. (b) Histogram of molecular orientations with respect to the normal of the {111}-facetted step as determined from an R-factor analysis. (c) Image part used for the R-factor analysis. For each molecule, the upper 16% of the histogram has been analyzed in order to avoid contributions of the local step geometry. Molecular orientations, as determined from this analysis, are indicated in the overview image. (d) R-factor values of all analyzed molecules.

the step edge (S or R),[22] which, in turn, depends on the small deviation of the step direction from $[0\bar{1}1]$. The choice of the appropriate surface orientation allows the selection of a single type of kink present at the surface.[23]

The asymmetric shape, in particular the apparent elevation of two of the six peripheral benzene rings, which is present in STM images, could be either related to a topographical effect (the adsorbed molecule is inclined on the step edge) or to an electronic effect (the electronic states of the metal surface are confined in the presence of the molecule, while the molecule itself is adsorbed on the lower terrace). In order to clarify this issue, we have performed ab initio calculations for five different configurations. These include (i) a molecule adsorbed on the free terrace, (ii) adsorption on the lower terrace close to the step, (iii) adsorption on the step, (iv) adsorption on the lower

(22) Ahmadi, A.; Attard, G.; Feliu, J.; Rodes, A. *Langmuir* **1999**, *15*, 2420−2424.
(23) Greber, T.; Šljivančanin, Ž.; Schillinger, R.; Wider, J.; Hammer, B. *Phys. Rev. Lett.* **2006**, *96*, 056103-1−056103-4.

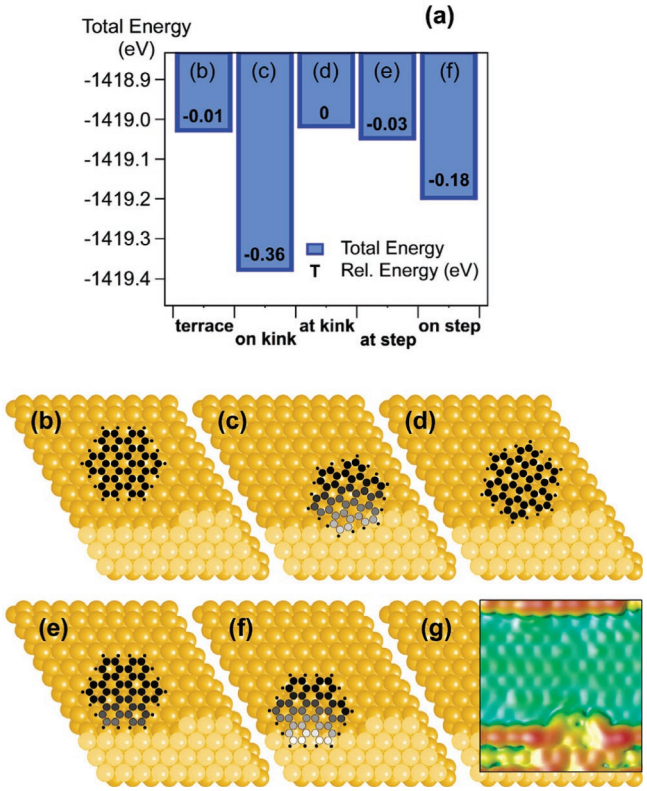

Figure 4. Ab initio calculations for HBC adsorption on Au(111). (a) Comparison of total energies for different relaxed adsorption geometries near a step defining a {100} microfacet. Relative energies are given inside the graph. (b)−(f) Relaxed unit cell geometries for adsorption on the free terrace, on the kink site, at the kink site, at a straight step edge, and on a straight step edge, respectively. The color-coded markers for the carbon atoms indicate the height with respect to the lower terrace (from black to white). (g) Charge-density distribution at the kink site (red is highest density).

terrace close to the kink site, and (v) adsorption on the kink site. The periodic Au unit cell in the simulations was large enough to accommodate all of the molecular configurations, and the calculated total energies could, thus, be directly compared. The system consisted of three Au layers, a kinked step, as well as the HBC molecule, with a total of 387 atoms in the unit cell. While the Au surface was frozen in the simulations, the HBC molecule was allowed to relax until the maximum residual force was <0.02 eV/Å. For the geometrical relaxation, a real-space grid with a plane-wave cutoff of 350 eV and the Γ-point in the reciprocal space were used.

Figure 4 (a) shows the total energies for HBC adsorption near a step defining a {100} microfacet. The energies for the different configurations vary significantly. First of all, adsorption sites where the molecule resides on a step or kink site are energetically more favorable than adsorption geometries where the molecule is adsorbed entirely on the lower terrace. This is in line with the experimental observation that, at low coverage, no molecules are observed on the terraces. The lowest energy is found for adsorption on a kink site (see Figure 4c for the adsorption geometry) with an energy gain of ∼0.4 and ∼0.2 eV with respect to flat adsorption geometries and adsorption on a straight step, respectively. The relaxed structure for "on-kink" adsorption reveals a tilted configuration with a height difference of 1.4 Å between the lowest and the highest carbon

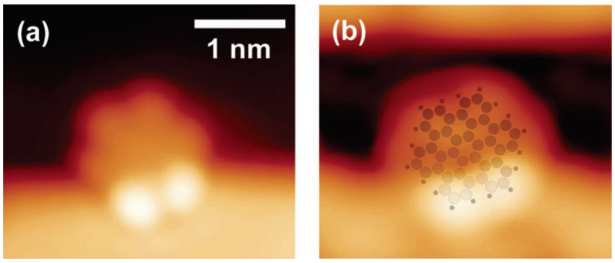

Figure 5. (a) STM image of an individual HBC molecule ($U = -0.2$ V, $I = 0.1$ nA). (b) Calculated STM image for the on-kink configuration (unit cell shown in Figure 4c) using the same sample bias. The increased height visible at the upper border of the image is due to the periodic boundary conditions used in the calculation and results from contributions of the step edge in the next unit cell.

atoms and an azimuthal angle of 17° between the mirror axis of the molecule and the normal of the step.

Figure 5 compares the measured STM image with the simulated image for the on-kink configuration. The simulated image confirms that the apparent hexagonal shape of the HBC molecule directly reveals the azimuthal orientation of the molecule. The agreement between measured and simulated images is excellent. In particular, the simulation reveals the same increased height on the two aromatic rings pointing to the upper terrace and an azimuthal orientation of the molecule that is identical to the one observed experimentally.

The lowest total energy and the excellent agreement between experimental and simulated STM images provide clear evidence for molecular adsorption on kink sites. It is thus clear that the observed height asymmetry is due to a truly topographic effect, that is, the molecule is adsorbed inclined over the kink site. In STM images simulated for the "at-kink" configuration (not shown), the height asymmetry is completely missing. This rules out the possibility that electronic coupling between the molecule and the upper terrace is responsible for the observed height asymmetry.

The on-kink configuration has also been analyzed for steps defining a {111} microfacet. The resulting relaxed structure for on-kink adsorption shows that the molecule has the same relative position with respect to the Au atoms of the upper terrace as that for the {100} microfacet. This, however, results in a different relative position with respect to the Au atoms of the lower terrace. Nevertheless, no significant difference is observed for the total energy between the two microfacets, indicating that the relevant structure for the energy gain and the molecular orientation for on-kink adsorption is the kink site defined by the upper terrace.

In contrast to the assumption of Weiss et al.,[24] we do not find strong dipolar interactions between the molecule and the step edge. At the Fermi level, the substrate density of states is substantially enlarged at the kink sites (Figure 4g), which explains the ground-state configuration by an enhanced overlap between surface electronic states and molecular states in this geometry. However, hybridization between surface and molecular electronic states is still comparatively weak, which indicates a lack of dipolar interactions and reveals that the molecules are physisorbed, rather than chemisorbed, on the kink, thus keeping the molecular states almost unperturbed.

(24) Weiss, P. S.; Kamna, M. M.; Graham, T. M.; Stranick, S. J. *Langmuir* **1998**, *14*, 1284−1289.

Conclusions

In summary, we have presented highly site-specific and single-orientation adsorption of HBC on monatomic steps of the Au(111) surface. The binding energies of HBC on the different stacking areas within the $22 \times \sqrt{3}$ superstructure of the Au(111) surface are sufficiently different to achieve selective adsorption on steps in fcc stacking regions. The selectivity in the adsorption orientation results from a binding energy on kink sites that is increased by 180 meV with respect to other adsorption geometries. The relaxed molecular structure has an angle of 17° with respect to the step normal, in excellent agreement with the experimental value of 18°. The results shown here indicate a promising route for the realization of supramolecular structures based on the controlled anchoring of molecular building blocks due to (i) the possibility to add a variety of functional side groups to the HBC core and (ii) the possibility to prepare regularly stepped Au surfaces with excellent long-range order. Regarding (ii), the successful preparation of the vicinal surfaces Au(788) and Au(11 12 12) has been reported,[5] providing two-dimensionally structured template surfaces consisting of regular step arrays in one and a periodic sequence of fcc and hcp stacking regions in the other direction.

Acknowledgment. Financial support by the European Commission (RADSAS, NMP3-CT-2004-001561) and the Swiss National Science Foundation (NCCR Nanoscale Science) is gratefully acknowledged.

JA0673231